Boletim da Sociedade Astronômica Brasileira, **35**, no. 1, 192-196

F-G dwarf stars hosting possibly rocky planets:

Key abundance ratios

M. Vieira & A. Milone

[1] Instituto Nacional de Pesquisas Espaciais
e-mail: matheus.vieira@inpe.br, andre.milone@inpe.br

Abstract. This study aims to identify chemical indicators related to the presence of rocky planets in F-G dwarf stars. Two samples were selected based on specific criteria, and analyses included distributions of abundance ratios, classification trees, linear discriminant analysis, and statistical tests for specific ratios. Sodium (Na) stands out as an indicator, while nitrogen (N) revealed unreliability. The ratios [Ni/Fe] and [C/O] emerge as subtle indicators, aligning with the results of the [E1/E2] versus [Fe/H] analysis from classification trees. The methods show a promising classification potential.

Resumo. Este estudo busca identificar indicadores químicos relacionados à presença de planetas rochosos em estrelas anãs F-G. Duas amostras foram selecionadas com base em critérios específicos, e análises abrangeram distribuições de razões de abundâncias, árvores de classificação, análise de discriminante linear e testes estatísticos para razões específicas. O sódio (Na) destaca-se como indicador, enquanto nitrogênio (N) revelou falta de confiabilidade. As razões [Ni/Fe] e [C/O] mostram-se como indicadores sutis, alinhando-se com os resultados da análise [E1/E2] versus [Fe/H] das árvores de classificação. Os métodos apresentam bom potencial classificatório.

Keywords. Stars: fundamental parameters – Stars: abundances – Stars: statistics

1. Introduction

With regard to the formation of stars and their planets, a fundamental characteristic associated with this is the primordial chemical composition of their gas and dust clouds. Since stars and their planets are formed from the same cloud, it is coMon to consider that the photosphere of main-sequence dwarf stars, which have not yet undergone changes due to evolutionary processes, acts as a fossil record of the chemical composition of the material from which the star formed.

According to the literature, stars hosting at least one giant gas planet are more abundant in iron compared to stars around which no planets have been detected. According to Fischer & Valenti (2005), the probability of a star hosting a giant gas planet is proportional to $10^{2[Fe/H]}$. However, such behavior is not exclusive to iron; it is shared by various other metals, such as alpha elements (Ne, Mg, Si, S, Ar, Ca, and Ti) and iron-peak elements (V, Cr, Mn, Fe, Co, and Ni) (da Silva, Milone & Rocha-Pinto (2015); Adibekyan et al. (2012); Gilli et al. (2006); Neves et al. (2009)). The mentioned characteristics are noticeable in Fig 1, where the small increase (especially in vanadium) in various elemental abundance ratios is evident for F-G-K dwarfs hosting giant gas planets (blue), compared to stars without detected planets (red).

The focus of this work is to attempt to identify good stellar chemical indicators that may be characteristic of the presence of rocky planets. A sample of main-sequence dwarfs from the solar neighborhood and members of the thin disk of the Galaxy, hosting possibly rocky planets, was selected for this purpose, along with a stellar sample of control dwarfs for comparison purposes. Various statistical methods were employed in a complementary manner, such as classification trees, linear discriminant analyses, and hypothesis tests for comparing sample means, along with kernel density distribution analyses. For these methods, a dataset in the space of abundance ratios involving elements from distinct groups related to the composition of rocky-metallic type planets was used.

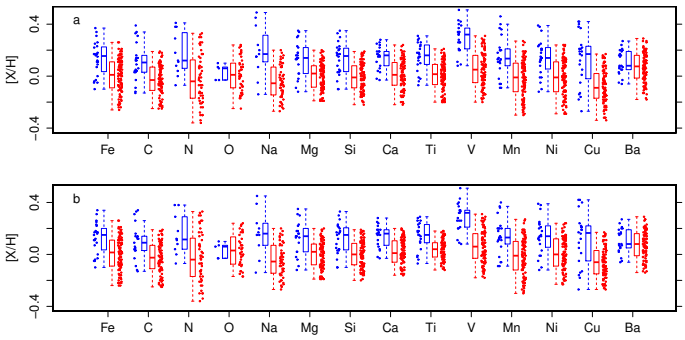

Figure 1. Boxplot for the comparison of elemental abundances [X/H] for 120 F-G-K dwarf stars in the solar neighborhood with and without planets, shown in blue and red, respectively. (da Silva, Milone & Rocha-Pinto (2015))

2. Sample selection

2.1. Study sample

Initially, we selected a sample of F-G-K-M dwarfs with metallicity around solar that hosted planets initially classified as "potentially" rocky. This initial selection was carried out using the planetary data repository from the NASA Exoplanet Archive (NASA). Table 3.1 outlines the filters used to obtain this initial sample.

We employed curves from planetary interior models (Zeng et al. (2019)) to narrow down the stellar sample to a metallicity range approximately 4 times the solar value. Using the curves from models of purely rocky (blue) and purely metallic planets (red), the broad sample of F-G-K-M dwarfs with planets, now referred to as possibly rocky planets, will include those dwarfs hosting planets whose masses and radii fall between these two curves, without taking into account the error in each of the two parameters (see Fig 2).

Table 1. Table listing the stellar and planetary filters used to obtain a broad sample of F-G-K-M dwarfs with metallicity around solar, hosts of potentially rocky planets.

Parameters	Filters	Range
Photospheric	T_{ef}(K)	[2500 , 6200]
	log g(g em cm.s^{-2})	[3,5 , 5,5]
	[Fe/H](dex)	[-0,66 , 0,66]
Planetary	R($R_\oplus$)	[0,5 , 5,0]
	M($M_\oplus$)	[0,3 , 100]
	ρ(g.cm^{-3})	$\geqslant 3,0$

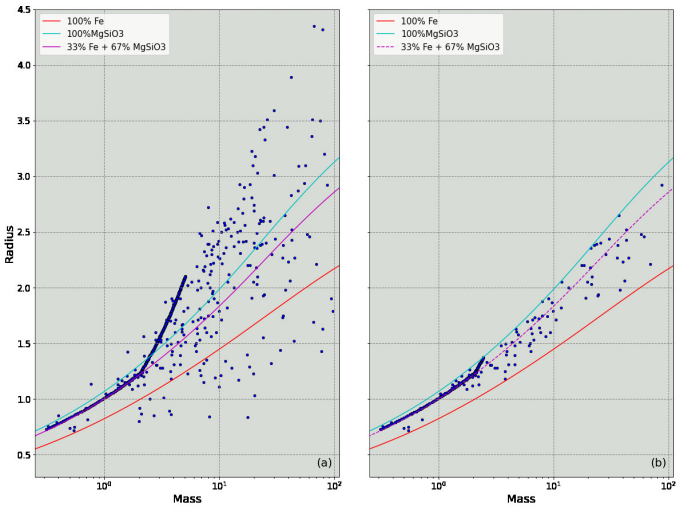

Figure 2. Mass-radius diagram, Planet Radius$_{planet}$ (linear scale in units of Earth's radius) versus Planet Mass$_{planet}$ (logarithmic scale in units of Earth's mass), (a) for the 1612 potentially rocky planets and (b) for the 641 possibly rocky planets from the broad stellar sample (F-G-K-M dwarfs hosting this type of planet and with metallicity $-0.66 \leqslant$ [Fe/H] $\leqslant +0.66$ dex). The planetary interior models of Zeng et al. (2016) for 4 different compositions are represented by the colored curves, as indicated in the internal legend of the graph.

We utilized the Hypatia catalog to gather dwarfs with cataloged stellar abundances. Among all stars containing abundances, we selected those exhibiting the highest ratios of coMon abundances within the photospheric temperature range. Subsequently, we conducted a kinematic classification using a Fortran code to minimize the effects steMing from the Galactic chemical evolution and to make the study sample of stars more homogeneous. Following this selection process, we obtained a study sample consisting of 160 F-G dwarfs from the thin disk, hosting possibly rocky planets.

2.2. Control sample

The control star sample was obtained from stars without detected planets in the Hypatia catalog. We selected stars within a range of photospheric parameters (T_{ef}, log g and [Fe/H]) equivalent to that of the current study sample. We obtained a total of 835 stars.

3. Results and discussions

3.1. Abundance distributions [X/H]

We compared the abundance distributions of 15 elements on the [X/H] scale between the d0 (without planets) and d1 (with planets) samples, represented by the red and blue colors, respectively (see Fig 3). The comparison reveals a subtle trend indicating that d1 stars exhibit slightly lower median abundances for all elements when compared to d0 stars. In other words, the box plot suggests that F-G dwarfs hosting planets likely tend to be less metal-enriched than stars without planets, in contrast to what is observed for stars hosting gas giant planets (Hinkel et al. (2019); da Silva, Milone & Rocha-Pinto (2015)).

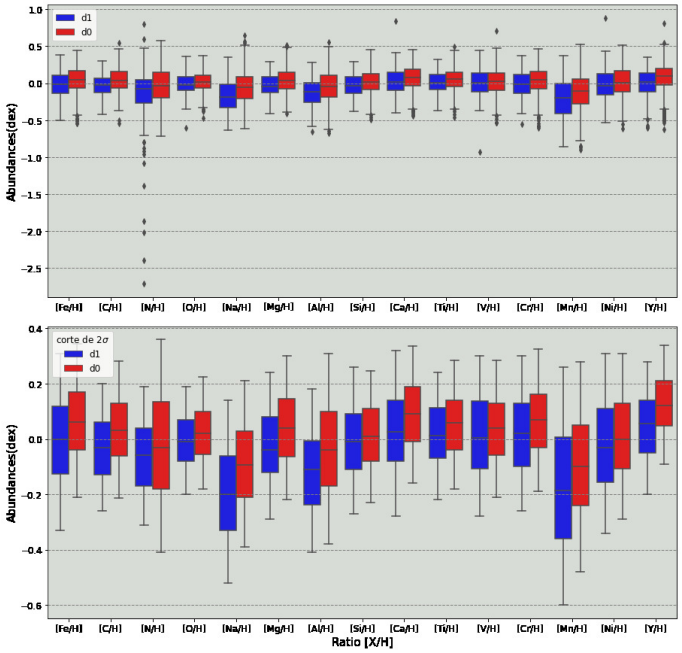

Figure 3. Boxplot for the comparison between elemental abundances of dwarf stars with possibly rocky planets and those with no detected planets, shown in blue and red, respectively.

3.2. Classification tree

To perform this analysis, a classification tree was applied to a comprehensive set of 15 [X/H] abundances (as shown in Figures 4 e 5) for the study sample (d1) in comparison with the control sample (d0). The panels (a), (c), (d), and (e) of Figure 4 present the classification trees for 4 groups of chemical elements: all 15 elements, volatiles, lithophiles, and siderophiles, respectively. Although the abundance space is composed of 15 distinct ratios, only 3 were necessary for good classification: N, Na, and Ti (Figure 4 (a)). However, by observing Figure 3, the excessive amount of outliers in nitrogen becomes evident. For this reason, the tree in Figure 4 (a) was not considered reliable, as we believe these outliers could be distorting the result in favor of nitrogen. Keeping this in mind, we chose to redo some classification trees by removing nitrogen (Figures 4 (b) and 5).

Based on the results presented in the classification trees, we can construct a table using the partition conditions of each tree. The aim is to examine abundance ratios in the [E1/E2] format that may be indicative of the presence of possibly rocky planets around their host stars. Thus, we present Table 2.

3.3. Linear Discriminant Analysis

An additional investigative approach to the study sample can be conducted through a Linear Discriminant Analysis (LDA). LDA

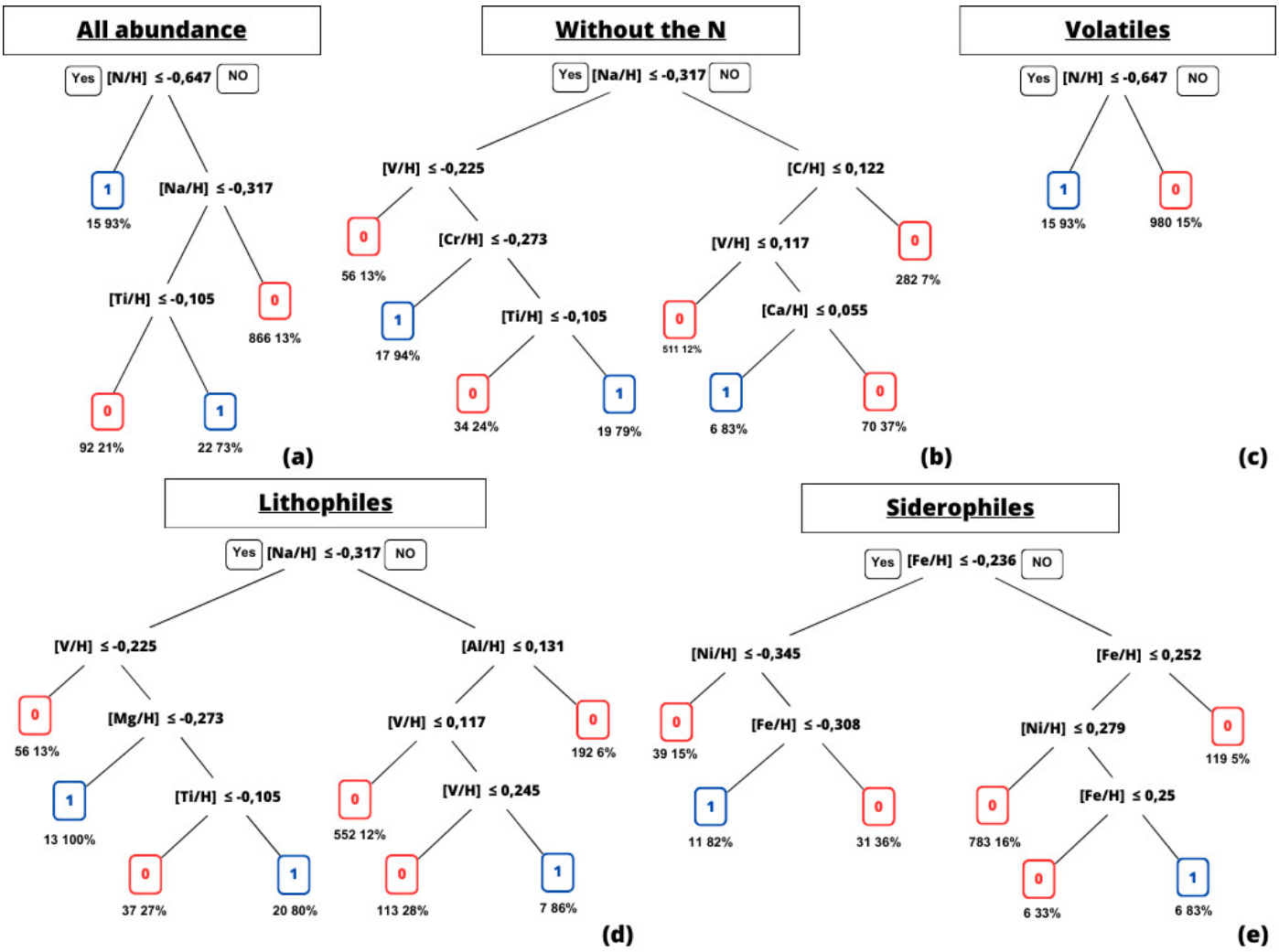

Figure 4. Classification trees were constructed based on the abundance space in the [X/H] format, with variables selected using the Gini metric. The variables for each classification are as follows: (a) all abundances, (b) all abundances except nitrogen, (c) volatile group, (d) lithophile group, and (e) siderophile group.

$cd_{(a)}$	d1(%) > cd	d1(%) ⩽ cd
$[V/Na]_{(b),(d)} > 0.09$	27	7
$[V/Cr]_{(b)} > 0.05$	32	12
$[Cr/Na]_{(b)} > 0.04$	20	7
$[Ti/Na]_{(b),(d)} > 0.21$	43	13
$[V/C]_{(b)} > 0.0$	23	10
$[V/Ca]_{(b)} > 0.06$	56	14
$[C/O]_{(c)} > 0.03$	20	12
$[V/Mg]_{(d)} > 0.05$	31	12
$[Mg/Na]_{(d)} > 0.04$	18	10
$[V/Al]_{(d)} > 0.11$	28	11
$[Ni/Fe]_{(e)} > -0.04$	20	9
$[Ni/Fe]_{(e)} > 0.03$	24	15

Table 2. (*a*): abbreviation for the condition, (*b*): all elements without N, (*c*): volatiles without N, (*d*): lithophiles, and (*e*): siderophiles.

is essentially a statistical method used to characterize or separate two or more distinct classes. This separation of classes is achieved by obtaining a linear combination of the observed properties that best discriminates between them. As a result, we obtain a coefficient or a set of coefficients that can serve as a linear classifier.

We applied LDA to the complete set of 15 abundance ratios of dwarf stars with the aim of finding the best linear combination capable of discriminating between samples d0 and d1. As a result, we obtained the indices presented in Table 3.

By performing a linear combination as described by Equation 1, where a_i represents the linear discriminant index associated with element X_i of a given star j, we obtain a set of values Z (where $Z = [Z_1, Z_2, \cdots, Z_j, \cdots, Z_n]$ for n stars) representing samples d0 and d1. Figure 6 presents histograms for the distributions of the variable Z for stars d0 and d1 (as this refers to the Z set, we will refer to it as Z0 and Z1 for stars d0 and d1, respectively).

$$Z_j = \sum_{i=1}^{n} a_i \left[\frac{X_i}{H}\right]_j \quad (1)$$

We employed the F-test for variance and the Welch's t-test to quantitatively assess whether the means and variances of these distributions are significantly different. As a result, it was statistically confirmed that the means and variances are distinct.

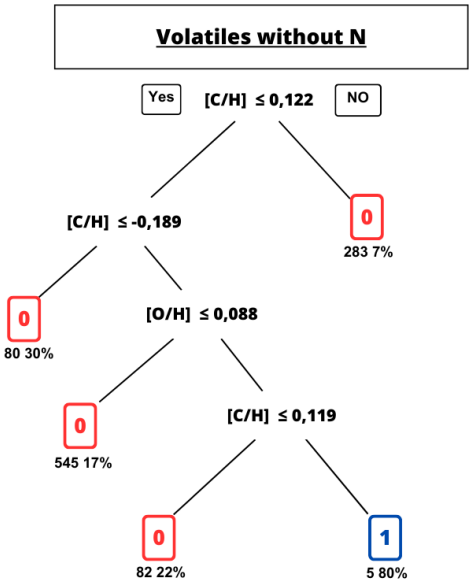

Figure 5. Classification tree constructed from the abundance space in the [X/H] format, with variables selected based on the Gini metric. The classification variables belong to the volatile group, excluding nitrogen.

Abundance ratio	Linear Discriminant
[Fe/H]	-20,052
[C/H]	-3,251
[N/H]	-2,098
[O/H]	3,108
[Na/H]	-11,162
[Mg/H]	-10,744
[Al/H]	-3,688
[Si/H]	10,436
[Ca/H]	-4,664
[Ti/H]	10,703
[V/H]	3,405
[Cr/H]	7,453
[Mn/H]	0,568
[Ni/H]	22,858
[Y/H]	-3,787

Table 3. Table of linear discriminant indices for abundance ratios obtained through LDA.

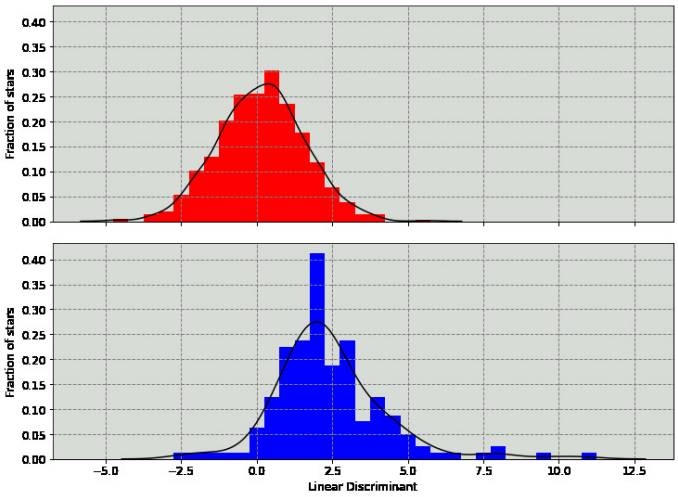

Figure 6. Histograms and kernel distribution of linear discriminant indices based on the indices defined in Table 3.

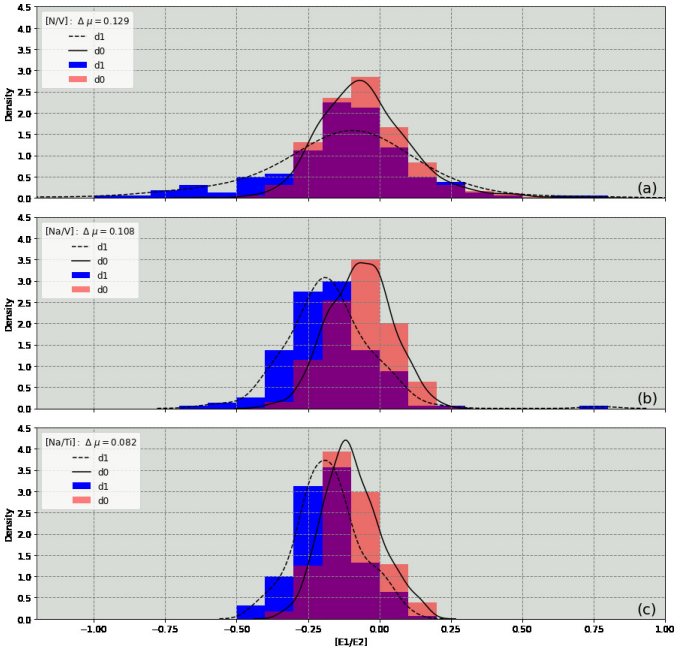

Figure 7. Histograms and kernel probability density functions for the relevant abundance ratios, [N/V], [Na/V], and [Na/V], selected by hypothesis tests.

3.4. Kernel density applied to [E1/E2] ratio distributions

From the 15 abundance ratios, we explored all combinations in the [E1/E2] format and selected, through hypothesis tests (mean and variance) and error analyses, the abundance ratios that showed significantly different means. Based on this criterion, we identified 3 abundance ratios: [N/V], [Na/V], and [Na/Ti]. Figure 7 presents the kernel distribution for these 3 abundance ratios, also including histograms for comparison purposes.

When comparing the kernel densities with their respective histograms, we can observe that the densities adequately represent the star distributions. The means of the distributions (indicated by triangles) are relatively close to the peak position, resembling a symmetric distribution around the mean, similar to a Gaussian distribution in most cases. However, when examining the [N/V] ratio plot, we notice that the kernel distribution for d1 stars is relatively different: the mean of the distribution is slightly farther from the peak position compared to the others, and the intersection of the histograms almost completely covers the two distributions. This is due to the presence of outliers in nitrogen, which may be influencing the result and consequently led the ratio to meet the criteria for statistical selection. We initially chose not to consider this ratio as relevant.

In the case of [Na/V] and [Na/Ti], although there is a considerable region of intersection between the distributions, these abundance ratios seem to be capable of efficiently distinguishing whether the stars are hosts to possibly rocky planets or not.

3.5. Abundance ratios versus presence of rocky planets

Figure 8 presents a set of stars with a slightly depleted [N/H] abundance, representing the outliers observed in Figure 3. This condition is also reflected in the classification tree in Figure 4(a), where [N/H] ⩽ -0.647 dex. The asymmetry in the distribution of nitrogen abundances for the d1 sample needs to be investigated

carefully to better understand why these values are so discrepant from the others.

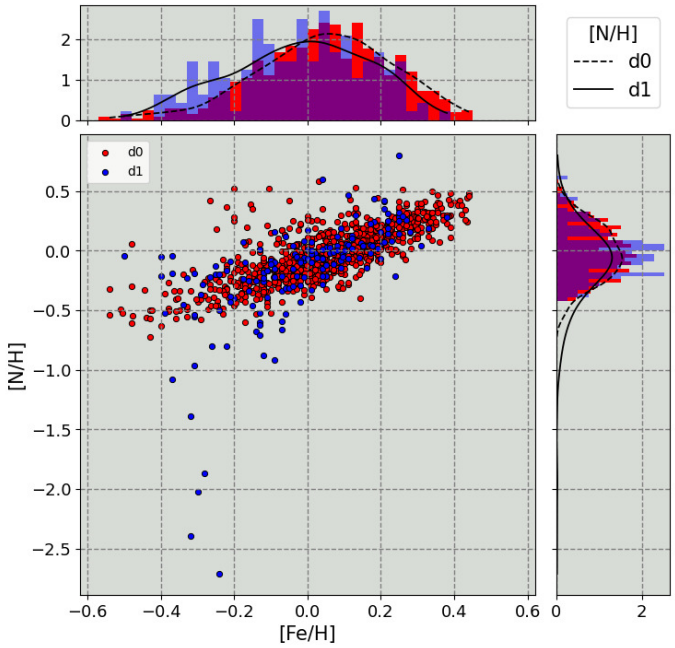

Figure 8. Set of plots of the [N/H] ratio as a function of [Fe/H]. The main panel displays a scatter plot of the distributions, while the secondary panels (along the axes) include histograms along with kernel density distributions. Identifications are provided in the figure captions.

Figure 9 presents a set of plots for some metal abundance ratios [E1/E2] versus [Fe/H], where these ratios are related to the composition of rocky planets: [C/O] (a ratio distinguishing carbon-rich planets when n(C)/n(O) > 0.8, from silicate and Mg-Si oxide-rich planets when n(C)/n(O) < 0.8 Bedell et al. (2018); Nissen & Gustafsson (2018)), [Mg/Si] (mineralogy), and [Ni/Fe] (a ratio associated with the composition of the core of rocky planets, such as metallic alloys, for example).

The distributions of the C/O ratio show comparable dispersions of values between the d1 and d0 samples, with the majority of stars in the d1 sample exhibiting n(C)/n(O) < 0.8. In the case of Mg/Si, both samples indicate that the majority of stars, both d1 and d0, have 1 < n(Mg)/n(Si) < 2. These facts suggest that both the d1 and d0 stars would be suitable sites to harbor or form rocky planets with Earth-like mineralogy.

Regarding the [Ni/Fe] ratio, we observe, based on the classification tree of siderophiles (see Table 2), that the presence of potentially rocky planets seemed to be indicated by a value around or above the solar ratio. Figure 9 emphasizes this, with the black bars precisely indicating the values of [Ni/Fe] obtained from the classification tree.

4. Conclusion

The study examined different abundance indicators in F-G dwarf stars hosting potentially rocky planets. A subtle trend was observed, suggesting that F-G dwarfs with rocky planets have slightly lower abundances of 15 metals ([X/H]) compared to those without detected planets, as evidenced by boxplots. The ratio [Na/H] was identified as a possible indicator of the presence of these planets, while the [N/H] ratio was initially not considered a reliable indicator.

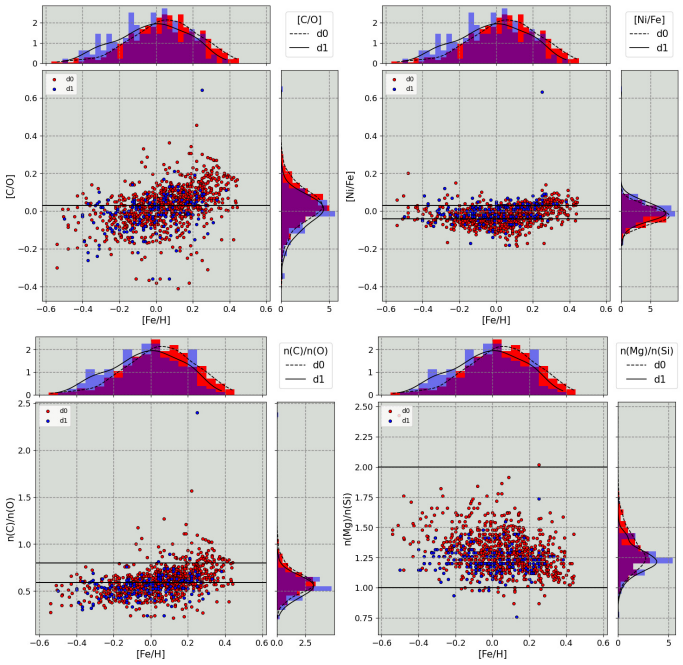

Figure 9. Multiple plots analogous to those in Figure 8 for [C/O] and its numerical scale ratio, the [Ni/Fe] ratio, and the numerical scale ratio of Mg/Si, all as a function of [Fe/H] for stars in d0 and d1.

Linear discriminant analysis suggested that the discriminants presented in the table could collectively serve as a good indicator of the presence of rocky planets in F-G dwarfs. Additionally, kernel estimate distributions revealed that the [Na/V] and [Na/Ti] ratios are good references for indicating F-G dwarfs hosting rocky planets.

Although the [N/V] ratio showed the largest difference between means, this difference was attributed to nitrogen, making it less reliable as an indicator. The ratios [Ni/Fe] and [C/O] were also identified as subtle indicators of the presence of rocky planets, based on the results of classification trees.

These findings point to potential chemical indicators that can be explored in future studies to better understand the relationship between chemical abundances in stars and the presence of potentially rocky planets.

References

Adibekyan, V. Zh., Santos, N. C., Sousa, S. G., Israelian, G., Delgado Mena, E., González Hernández, J. I., Mayor, M., Lovis, C. & Udry, S. 2012., Astronomy & Astrophysics 543, A89.

Bedell, M., Bean, J. L., Meléndez, J., Spina, L., Ramírez, I., Asplund, M., Alves-Brito, A., dos Santos, L., Dreizler, S., Yong, D., Monroe, T., Casagrande, L. 2018, The Astrophysical Journal, 865(1), 68.

da Silva, R., Milone, A. de C. & Rocha-Pinto, H. J. 2015., Astronomy & Astrophysics, 580, A24.

Fischer, D. A. & Valenti, J. 2005, The Astrophysical Journal, 622(2), 1102.

Gilli, G., Israelian, G., Ecuvillon, A., Santos, N. C. & Mayor, M. 2006. Astronomy & Astrophysics, 449(2), 723-736.

Hinkel, N. R., Unterborn, C., Kane, S. R., Somers, G. & Galvez, R. 2019, The Astrophysical Journal, 880(1), 49.

Nissen, P. E. & Gustafsson, B. 2018, The Astronomy and Astrophysics Review, 26(6), 1.

Neves, V., Santos, N. C., Sousa, S. G., Correia, A. C. M. & Israelian, G. 2009. Astronomy & Astrophysics, 497(2), 563.

Zeng, L., Jacobsen, S. B., Sasselov, D. D., Petaev, M. I., Vanderburg, A., Lopez-Morales, M., Perez-Mercader, J., Mattsson, T. R., Li, G., Heising, M. Z., Bonomo, A. S., Damasso, M., Berger, T. A., Cao, H., Levi, A. & Wordsworth, R. D. 2019, Proceedings of the National Academy of Sciences, 116(20), 9723.